Review of Plasma-Induced Hall Thruster Erosion

Nathan P. Brown [1],* and Mitchell L. R. Walker [2]

[1] Graduate Fellow, Aerospace Engineering, Georgia Institute of Technology, Atlanta, GA 30332, USA

[2] Professor and Associate Chair, Aerospace Engineering, Georgia Institute of Technology, Atlanta, GA 30332, USA; mitchell.walker@ae.gatech.edu

* Correspondence: nbrown44@gatech.edu

Abstract: The Hall thruster is a high-efficiency spacecraft propulsion device that utilizes plasma to generate thrust. The most common variant of the Hall thruster is the stationary plasma thruster (SPT). Erosion of the SPT discharge chamber wall by plasma sputtering degrades thruster performance and ultimately ends thruster life. Many efforts over the past few decades have endeavored to understand wall erosion so that novel thrusters can be designed to operate for the thousands of hours required by many missions. However, due to the challenges presented by the plasma and material physics associated with erosion, a complete understanding has thus far eluded researchers. Sputtering rates are not well quantified, erosion features remain unexplained, and computational models are not yet predictive. This article reviews the physics of plasma-induced SPT erosion, highlights important experimental findings, provides an overview of modeling efforts, and discusses erosion mitigation strategies.

Keywords: electric propulsion; Hall thruster; stationary plasma thruster; sputtering; erosion

1. Introduction

The Hall thruster is a spacecraft propulsion device that generates thrust via electrostatic acceleration of plasma ions. Figure 1 shows a Hall thruster operating in the High-Power Electric Propulsion Laboratory at the Georgia Institute of Technology.
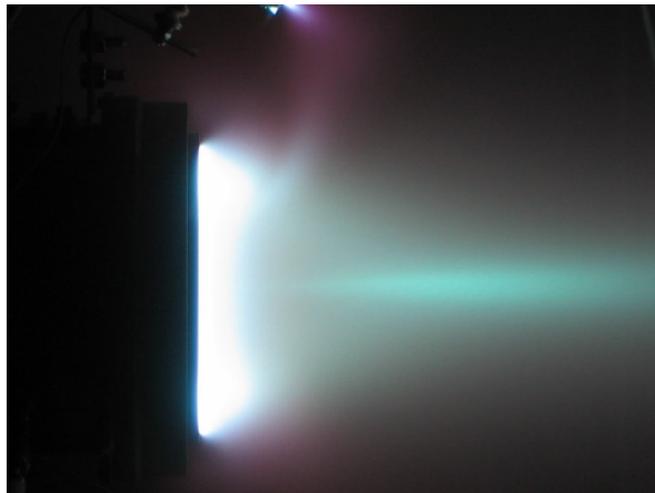

Figure 1. Pratt & Whitney T-140 Hall thruster operating with xenon propellant.

Performance varies across design and power class, but typical thrusters have a demonstrated lifespan on the order of 10,000 h and produce 0.1–1 N of thrust with a specific impulse (total imparted momentum per unit weight of propellant) of 1000–3000 s [1–8]. These characteristics have made the Hall thruster a leading propulsion option for both satellite station-keeping and deep-space exploration. Hall thrusters have flown on hundreds of spacecraft since the 1971 launch of the Russian METEOR-18; they presently provide orbit corrections for the SpaceX Starlink constellation and are scheduled to serve as primary propulsion elements for both the NASA Psyche and Artemis missions [9–11].

The most common variant of the Hall thruster, called the stationary plasma thruster (SPT), ignites and sustains plasma within a discharge chamber composed of ceramic walls. Hall thruster erosion is the gradual removal of ceramic material from the discharge chamber walls by plasma sputtering. Total removal of the ceramic results in exposure of magnetic circuitry components to plasma and effectively ends thruster life [2,5,12,13]. Wall material removal also impacts thruster performance well before the end of life is reached. Thruster life tests have shown that thrust and specific impulse can decrease by 5–8% over the first 1000 h of operation, when the erosion rate is highest [14–20].

Erosion is a plasma–material interaction that forms a coupled feedback loop; sputtering alters wall surface properties, which leads to changes in plasma boundary conditions that, in turn, adjust the discharge sputtering rate. Further complications arise due to the high sensitivity of sputtering to both surface and plasma conditions. Despite substantial efforts to experimentally measure and computationally model the process, many aspects are not well understood. The sputtering rate of the ceramic discharge chamber walls has not been adequately quantified, the connection between erosion and performance degradation requires further study, and an explanation of the ubiquitous presence of so-called "anomalous" erosion ridges in thruster life tests has remained elusive.

The purpose of this review is to introduce the reader to the unique challenges presented by plasma-induced Hall thruster erosion and to overview experimental and computational studies on the topic. Section 2 introduces erosion physics, Sections 3 and 4 highlight experimental and modeling efforts, respectively, and Section 5 discusses erosion mitigation concepts. Unless otherwise noted, Hall thruster is used synonymously with SPT in this review.

2. Physics of Hall Thruster Erosion

Hall thruster erosion is the gradual removal of material from the ceramic walls of the discharge chamber via plasma sputtering. Wall erosion eventually exposes magnetic circuitry components to plasma and effectively ends thruster life. This section provides an overview of Hall thruster plasma, discharge chamber wall materials, and sputtering.

2.1. Hall Thruster Plasma

Shown schematically in Figure 2, the Hall thruster forms and sustains plasma with crossed electric and magnetic fields within an annular ceramic discharge chamber. An external power supply establishes an electric field along the discharge axis, and a set of solenoids generates a magnetic field that points along the discharge radius. The electric field is established between a positively biased anode and a negatively biased emitting hollow cathode. The crossed electric and magnetic fields force electrons emitted by the cathode into a gyrating azimuthal Hall drift inside the discharge chamber. Neutral propellant (typically xenon) fed through the anode collides with the electrons to form ions that are subsequently accelerated into the thruster exhaust by the axial electric field. Charge quasineutrality is maintained in the resulting plume because some emitted electrons follow expelled ions rather than enter the discharge chamber. The ionized propellant is not captured in a Hall drift inside the discharge chamber because, though large enough to magnetize electrons, the magnetic field does not have sufficient strength to magnetize the comparatively heavy ions [1–8].
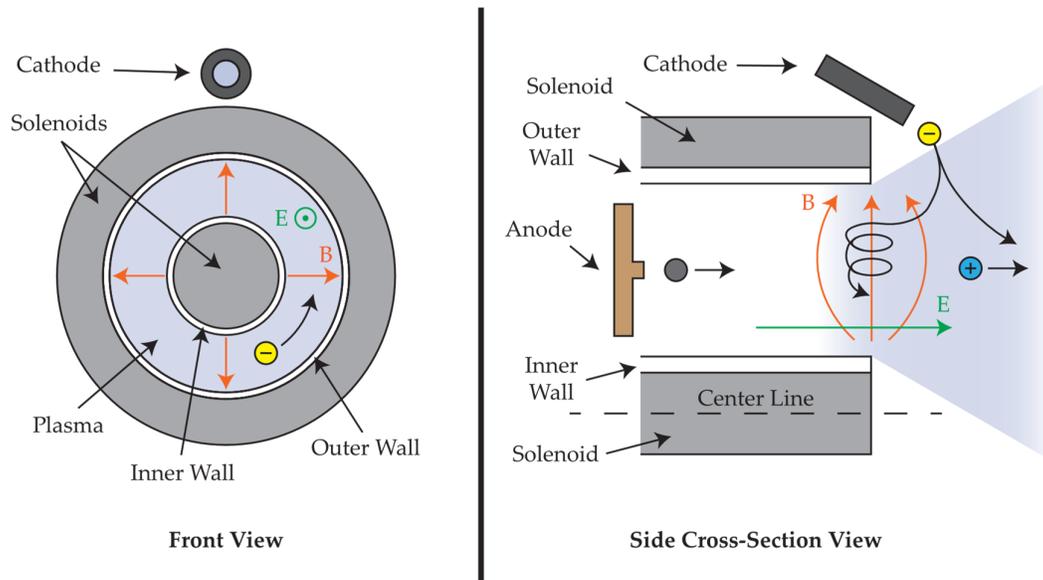
Figure 2. Front and side cross-section schematics of a Hall thruster [3,7]. Electrons (yellow) trapped in a Hall drift by crossed electric (green) and magnetic (orange) fields ionize neutral (grey) propellant. The resulting ions (blue) are accelerated into the thruster plume by the electric field.

Representative peak electric and magnetic field values inside the discharge chamber are 400 V/cm and 200 G, respectively. The plasma density is typically 10^{17}–10^{19} m^{-3}, electron temperature generally remains below 100 eV, and the peak ionization fraction exceeds 10%. The ion-neutral collision frequency is on the order of 10–100 kHz, and the total electron collision frequency is 1–10 MHz [3,6,7,21].

Erosion rates are greatest near the thruster exit plane in the so-called propellant ionization and ion acceleration zones, where ion density and energy are largest due to axial peaks in the electric and magnetic fields [7,22,23]. The radial distribution of the electric field in these regions is influenced by the magnetic field configuration, discharge chamber wall boundary conditions, charged particle densities, and plasma turbulence [7,8]. These factors complicate the idealized scenario presented in the preceding description and can cause ions to accelerate into the walls of the discharge chamber, rather than into the thruster plume. Estimates vary, but some work has shown that as many as 30–40% of Hall thruster ions are accelerated into the thruster walls [5].

A substantial source of this wall acceleration is the plasma sheath that forms to connect the quasineutral bulk plasma to the discharge chamber walls. Because the walls are insulating, the sheath must form to enforce a zero net current boundary condition at the wall. Electrons reach the wall first, so the sheath resists further electron current to the wall by establishing a potential drop from the bulk plasma to the wall. Ions formed sufficiently close to the wall or transported to the wall region by collisions or local electric fields are accelerated into the wall by the sheath potential gradient [7,8,24,25]. Figure 3 provides a simplified illustration of this effect.
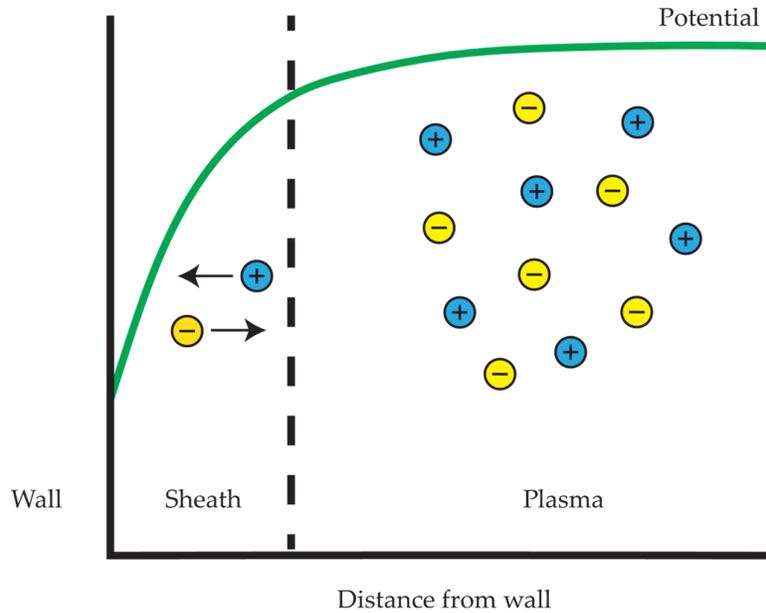
Figure 3. Simplified illustration of the potential drop in the wall sheath [24]. The potential gradient in the sheath repels electrons (yellow) away from the wall and accelerates ions (blue) toward the wall.

2.2. Discharge Chamber Wall Material

Hall thrusters require ceramic discharge chamber walls to protect the solenoids from plasma exposure. Selection of wall material can impact thruster performance and operating conditions. The material must have low electrical conductivity at high temperatures, high mechanical strength, good thermal shock resistance, low outgassing rate, low secondary electron emission rate, and low sputtering yield [12,26,27]. Boron nitride–silica (BN-SiO$_2$) composite is the most commonly reported flight thruster wall material, but alumina (Al$_2$O$_3$), silicon carbide (SiC), and various grades of BN featuring different binder materials have been used in laboratory thrusters [28].

BN-SiO$_2$ composite is formed by hot-pressing hexagonal BN platelets in amorphous SiO$_2$ binder. The resulting composite is orthotropic because properties along directions parallel to the platelet plane differ from properties along the platelet normal [29–31]. Figure 4 is a scanning electron microscope (SEM) image of grade M26 BN-SiO$_2$ composite taken without the aid of conductive surface coating. The fibrous appearance of the BN grains is due to the on-edge view of the BN platelets.
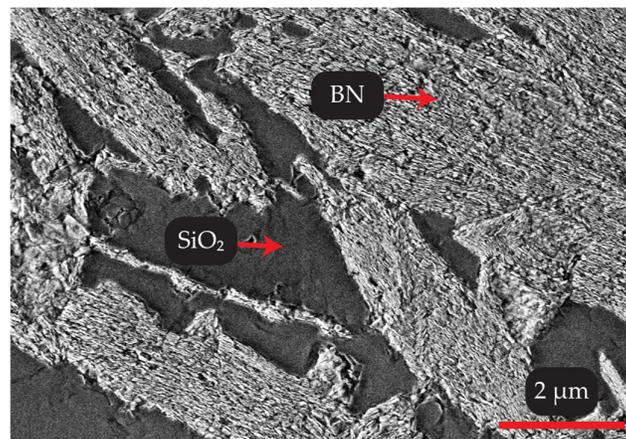

Figure 4. Scanning electron microscopy (SEM) image of grade M26 BN-SiO$_2$. The dark regions are amorphous silica (SiO$_2$) and the light regions are orthotropic boron nitride (BN).

2.3. Sputtering

Hall thruster erosion is the gradual sputtering of the discharge chamber walls. Sputtering is the ejection of atoms from a material surface by incident energetic particles. The process is important for many applications and is used as a tool for thin film sputter deposition, ion beam etching, and secondary ion mass spectrometry [32,33]. One such application, planar magnetron sputter deposition, involves sputtering of a material target with plasma that, as in a Hall thruster, is formed and sustained by crossed electric and magnetic fields [34]. The advancement of sputtering applications has benefited Hall thruster erosion research because much of the development of sputtering theory has been motivated by these fields.

Sputtering is prevalent in plasma-material interactions because many plasmas consist of particles with sufficient energy to release atoms from material surface bonds. These particles can be neutrals, ions, or electrons, but ions with energies below 500 eV are widely expected to be the primary agent of sputtering in the case of Hall thruster wall erosion [35–37]. Researchers quantifying sputtering for Hall thruster wall materials typically report sputtering rate (or yield) as the measured ejected surface material volume per time-integrated incident ion current, resulting in dimensions of volume per electric charge [35,38–40]. However, in other fields, the sputter rate is often given as the average number of surface atoms ejected per incident ion [32,33].

The transport model provides a satisfactory conceptual picture of the mechanism by which sputtering takes place. Transport theory holds that sputtering happens in three main stages: (1) incident energetic particles transfer energy to material atoms through collisions, (2) impacted material atoms transfer energy to other material atoms in a collision cascade, and (3) some atoms near the material surface gain sufficient velocity in a direction pointing away from the surface to leave the material altogether [32,33]. Figure 5 illustrates the transport theory sputtering mechanism.
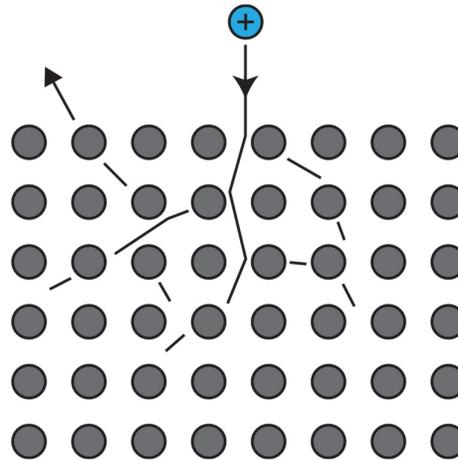

Figure 5. Sputtering mechanism according to the transport model [33]. An incident ion (blue) transfers energy to atoms (grey) and the resulting collision cascade propels an atom away from the surface.

Application of the transport model results in a simple relation for the sputter yield that can be corrected for many different materials exposed to a variety of plasma species. The model is fundamentally limited, however, because it assumes the material is a homogenous continuum and relies on adjustable parameters for fitting to experimental data. Sputtering is a far more complex process than what is implied by the transport theory. The sputtered material may have heterogeneous structure, sufficiently high temperatures can cause material sublimation, incident particles may not immediately collide with surface atoms due to ion and energy channeling, and adatom-vacancy pairs and surface island nucleation may form due to energetic atoms not leaving the material surface. These shortcomings may be overcome by individually computing particle trajectories with molecular dynamics simulations [32,33,41].

Propulsion engineers must accurately model Hall thruster wall sputtering to predict Hall thruster wall erosion rates and determine the resultant thruster lifetime. This task is challenging because the sputtering rate is highly sensitive to surface properties, such as temperature, roughness, contamination, and charge, and near-wall plasma properties, such as ion density, energy, and incidence angle [32,33]. To make matters even more complicated, sputtering of the Hall thruster wall changes the surface composition and secondary electron yield. These changes, in turn, alter both the material and plasma properties [22,23,39,42,43]. The result is a coupled feedback loop, whereby sputtering of the thruster wall changes the sputtering rate. Experimental and computational work in the field over the last few decades has been driven by the need to understand both the wall material and plasma to enable an accurate description of how these two entities interact.

3. Experimental Investigations of Hall Thruster Erosion

Experimental investigations of Hall thruster erosion can be broadly grouped into two categories: thruster tests and material surface investigations. Thruster tests provide overall erosion and performance characteristics, whereas material surface investigations study sputtering yield and the impact of sputtering on surface structure. This section highlights important results found in both investigation types.

3.1. Thruster Tests

The Fakel SPT-70 and SPT-100 Hall thrusters successfully operated on Soviet Union satellites in the 1970s and 1980s, but interest in lifetime tests was renewed in the early 1990s as the life of geostationary spacecraft improved and thruster life requirements grew from 700–2000 h to 4000–6000 h [12]. Early available data on thruster erosion therefore comes from workers in the United States and the former Soviet Union states attempting to qualify the 1.35 kW SPT-100 for longer-term operation with xenon propellent.

The SPT-100 discharge chamber has a length of 2.5 cm, inner radius of 3.5 cm, and outer radius of 5 cm, resulting in a total discharge chamber volume of approximately 100 cm^3 [7]. The initial thicknesses of the inner and outer annulus walls are approximately 11 mm and 5.5 mm, respectively [14,15]. Erosion rates were reported as the loss of thickness or volume per unit time and were determined by periodically measuring changes in either the wall thickness or mass. Four notable results were garnered from these tests. First, erosion was most prominent in the 10 mm closest to the thruster exit plane (where ionization and ion acceleration are most prevalent). Second, the erosion rate decreased exponentially with time from ~10 μm/h to ~1 μm/h. Third, the outer wall eroded more rapidly than the inner wall. Fourth, thrust and specific impulse decreased by 5–8% over the first few hundred hours of thruster operation, and discharge electrical oscillations were not consistent throughout thruster life [14,15,44].

Later tests of the Keldysh Research Centre 1.3 kW T-100 [45] and KM-series thrusters [19], Snecma 1.3 kW [16,17] and 2.5 kW [20] variants of the PPS-1350, Pratt & Whitney 10 kW T-220 [46], NASA 50 kW T-400M [47], and Aerojet Rocketdyne 4.5 kW BPT-4000 [18] found similar trends in erosion rate and performance loss but did not universally observe more rapid erosion of the outer wall. The T-220 campaign reported variation of erosion rate with azimuthal position, and the BPT-4000 test campaign measured no erosion after 5600 h of operation. The BPT-4000 result was explained as a "magnetic shielding" effect and led to the development of the Zero-Erosion™ thruster line [48].

Hall thrusters are typically operated and characterized with xenon propellent. Assessment of the impact of alternative propellants on the SITAEL 5 kW HT5k performance found that use of krypton and krypton-xenon mixtures, compared to pure xenon, resulted in higher wall erosion rate [49]. Other efforts have quantified wall erosion in thrusters operating with krypton propellent, but more work is required to compare krypton and xenon erosion trends and to understand the erosion characteristics of other alternative propellants, such as argon and iodine [47,50].

Other notable work to experimentally characterize plasma-induced erosion in Hall thrusters includes that of Peterson et al. [51], who tested the relative erosion rates of Hall thruster channels constructed from various grades of BN composites, and Bugrova et al. [52], who found erosion rate

increases with discharge voltage. The importance of pressure facility effects on erosion rate was recently examined by Zhang et al. [53] and Ortega et al. [54]. In parallel, other researchers [46,55–64] have developed in-situ erosion rate measurement techniques, such as telemicroscopy and spectroscopy.

The most surprising erosion result from thruster life tests is the formation of mm-scale sawtooth erosion patterns in both the inner and outer annulus walls. First reported in the literature by Arhipov et al. [65], so-called anomalous erosion ridges are a ubiquitous presence in Hall thruster walls and can be detected after fewer than 100 h of operation [13]. Erosion ridges are clearly discernable in Figure 6, for example, which shows the BPT-4000 [18], PPS-1350 [66], and SPT-100 [15] after life tests. The cause of erosion ridges is not known, but work has attempted to link their formation to both plasma and material instabilities [67–69].
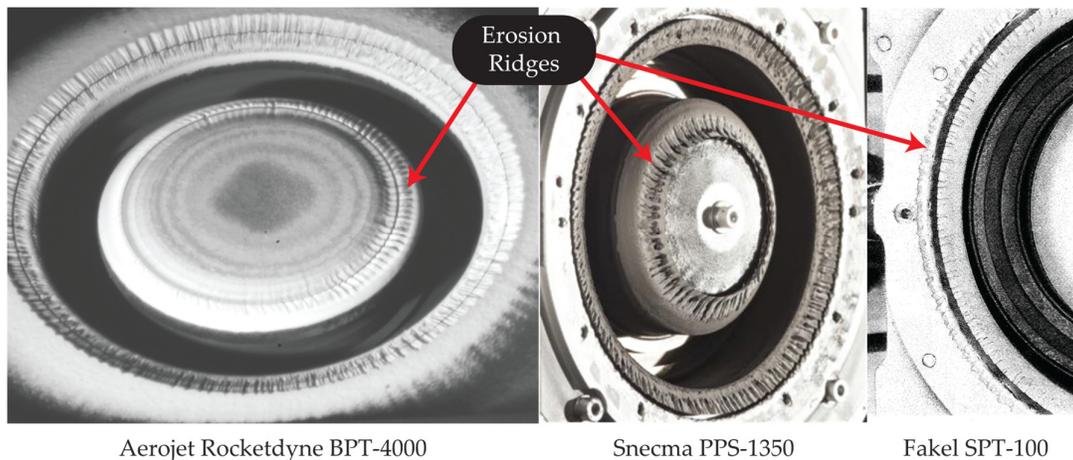

Aerojet Rocketdyne BPT-4000   Snecma PPS-1350   Fakel SPT-100

Figure 6. Erosion ridges in the Aerojet Rocketdyne BPT-4000, Snecma PPS-1350, and Fakel SPT-100 walls. Images reprinted with permission from [18], Aerojet Rocketdyne, 2010; with permission from [66], Snecma, 2019; and with permission from [15], American Institute of Aeronautics and Astronautics, 1995.

The mechanism behind the observed exponential decrease in erosion rate is also not completely understood. Erosion causes the walls to recede and thereby increases the volume of the discharge chamber; the larger volume may increase the probability that energetic ions collide with other particles and lose energy before striking the wall [70]. Changes to the ion incidence angle due to the surface response to sputtering may also act to reduce the erosion rate [71].

The decrease in performance over the first 1000 h of operation has been linked to multiple causes. The increase in discharge chamber volume may decrease the ion density or increase the plume divergence sufficiently to reduce thrust [37]. Sputtered wall material can also coat the anode and enter the plume, which may impact discharge electrical characteristics [72–74]. Shagaida et al. [19] proposed that erosion can lead to an increased proportion of non-propellant neutral particles in the discharge chamber and that this decreases thruster performance by lowering propellant utilization efficiency.

3.2. Surface Investigations

The presence of unexplained erosion features prompted Zidar and Rovey [22] and Burton et al. [23] to investigate the microstructure of eroded laboratory Hall thruster walls. These studies found the presence of striations on the order of the electron gyroradius and surface damage in the form of delamination and microcracking. Though they observed opposite trends in relative sputtering rates of BN and SiO_2 in BN-SiO_2, both studies found that original compound atomic ratios were not maintained in highly eroded regions; the ratio of B to N atoms was not 1:1, and the ratio of Si to O atoms was not 1:2. These results indicate that sputtering occurs on an atomic, rather than molecular, level in the Hall thruster wall.

Figure 7 shows an SEM image of grade M26 BN-SiO₂ after exposure to plasma, taken without the application of a conductive surface coating. Microcracks and striations are observable in the image, and BN delamination prevents discernment of BN grain boundaries.
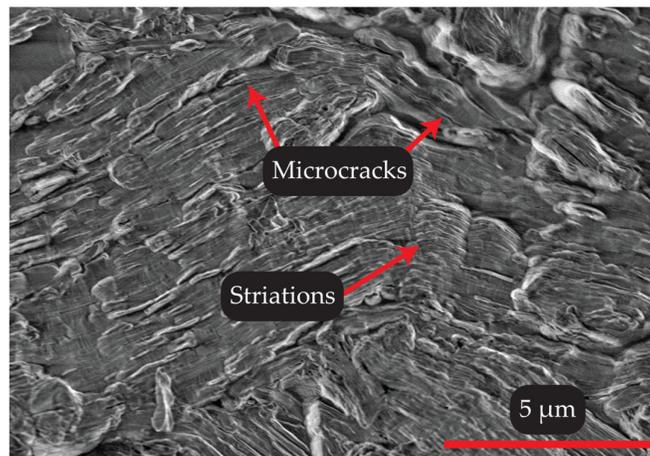

Figure 7. SEM image of grade M26 BN-SiO₂ after exposure to plasma. Comparison with Figure 4 demonstrates the change in surface microstructure caused by sputtering.

Recent work has used controlled experiments to investigate sputtering mechanisms and isolate the impact of specific factors on sputtering characteristics. Duan et al. [75] found that sintering pressure can impact BN erosion characteristics and that BN sputtering results in the breaking of B–N bonds and delamination of BN layers. Surface composition analysis showed that boron sputters more quickly than nitrogen when BN is exposed to xenon plasma. Satonik et al. [76] exposed pristine and Hall thruster-eroded BN and BN-SiO₂ samples to xenon magnetron plasma and found that previously eroded samples sputtered up to 90% faster than pristine samples. Their work found conflicting results regarding the relative sputtering rates of BN and SiO₂ in BN-SiO₂ but confirmed that compound atomic ratios were not maintained. Schinder et al. [69] attempted to explain the formation of anomalous erosion ridges in BN-SiO₂ with surface instabilities driven by hoop stresses, but experimental results failed to support this hypothesis. Experimental evidence for the role of electrons in the Hall thruster erosion process was provided by Sarrailh et al. [77], who exposed BN-SiO₂ and BN to both electron and ion beams. Brown et al. [42] demonstrated that microcracks observed in BN-SiO₂ thruster walls were caused by thermal shock induced by thruster on/off cycling but did not find that cracking influenced erosion characteristics. X-ray photoelectron spectroscopy data and SEM images from their work supported the notion that SiO₂ is sputtered more quickly than BN.

An important subset of surface investigations has attempted to quantify the low-energy sputtering yields of Hall thruster wall materials. Sputtering rates of BN and BN-SiO₂ at ion energies relevant to Hall thruster erosion (<500 eV) are vital for erosion models, so the Hall thruster community has attempted to measure these values in controlled experiments. Garnier et al. [38,39] determined angle-dependent sputtering rates of these materials by measuring sample mass loss after exposure to xenon plasma with mean ion energies of 350 eV, 500 eV, and 1000 eV. Their work found BN-SiO₂ sputtered at a greater rate than BN but that the relative sputtering rate of BN was larger than SiO₂ in BN-SiO₂. Curiously, their work also found that the atomic ratios of B to N and Si to O remained 1:1 and 1:2, respectively, in contrast to the results of later thruster and controlled sputtering tests performed by other authors [22,23,42,75,76]. Kim et al. [78] found that krypton plasma sputtered BN-SiO₂ at a 30–50% lower rate than xenon plasma at mean ion energies ranging from 100 to 400 eV. Rubin et al. [35] used quartz crystal microbalance and weight loss measurements to determine the angle-dependent sputter yields of different grades of BN with mean xenon ion energies ranging from 60 to 500 eV. Ranjan et al. [40] provided similar measurements for both BN and BN-SiO₂.

Due to difficulties associated with the determination of low-energy sputtering yields, substantial variation exists among sputtering yield datasets. More work is therefore needed to provide accurate quantification of atomic sputtering yields at low ion energies. Success in this endeavor will require the development of higher fidelity sputtering yield measurement tools, stable low ion energy plasma sources, and methods to accurately simulate the Hall thruster discharge in a controlled laboratory setting.

4. Hall Thruster Erosion Modeling

Predictive Hall thruster erosion modeling is a formidable challenge that promises to enable researchers to accurately and rapidly assess the lifetime of thruster prototypes without the need for expensive and time-consuming life tests. However, predictive modeling requires a precise description of the discharge plasma, wall material, and plasma-wall interaction, as well as the ability to simulate the impact of microsecond-scale events over the course of thousands of hours. Experimental uncertainties in available experimental data and limitations in computing power have thus far prevented the development of truly predictive models. Though they can accurately reproduce the decaying erosion rate trend observed in Hall thruster life tests, most contemporary models are highly sensitive to tunable parameters that must be adjusted to match preexisting thruster erosion data. They are also unable to reproduce experimentally observed surface evolution features, such as anomalous erosion ridges, microcracking, and atomic-level changes in surface composition. This section reviews erosion modeling and highlights important results.

Early efforts [79,80] circumnavigated the need for detailed plasma and sputtering models by simply curve-fitting preliminary SPT-100 erosion data to extrapolate erosion trends and thereby predict thruster life without complete life test data. Though recent work [81] has improved upon this technique by employing machine learning across multiple thruster life test datasets, life test data extrapolation is a fundamentally limited approach. It requires a thruster be constructed and operated before any life prediction is made and therefore does not enable rapid assessment of multiple thruster prototypes in early design stages.

More sophisticated models introduced by Komurasaki et al. [82] and Clauss et al. [83] in the late 1990s used fluid equations to describe the plasma discharge and determine the ion flux to the wall. The ion wall flux, coupled with a simplified sputtering rate model, gave a first-order calculation of erosion rate. The sputtering rate model used by these authors is given in Equation (1), where Y is the sputtering rate, J_i is the ion current density to the wall, and S is a sputtering factor that incorporates dependence on ion energy and angle of incidence.

$$Y = J_i S \tag{1}$$

Later efforts [70,84–91] accounted for plasma–wall interactions and implemented increasingly sophisticated discharge plasma and semiempirical sputter yield models tethered to experimental data. Many authors fit variations of the Yamamura and Tawara [92] sputtering rate law for monoatomic solids to the sputtering rate data of Garnier et al. [38,39] or Rubin et al. [35]. The general Yamamura and Tawara model is given in Equation (2), where F is a function that describes the dependence of sputtering rate on wall material and ion properties, E is ion energy, E_{th} is the threshold sputtering energy of the wall, and b is an adjustable parameter.

$$Y = F(\dots)\left(1 - \sqrt{\frac{E_{th}}{E}}\right)^{b} \tag{2}$$

Threshold sputtering energy is typically assumed to lie between 30 and 70 eV. The form of Equation (2) and the values of the associated fit parameters vary as a function of the chosen model, fitted experimental data, and assumed threshold sputtering energy.

An important contribution was made by Manzella et al. [70], who recovered the exponentially decaying erosion rate observed in life tests by updating the thruster discharge size with wall erosion. Increased discharge volume caused by decreased wall thickness provided ions with greater

opportunity to collide and lose energy before striking the wall, thereby decreasing the sputtering rate. The model of Sommier et al. [37] reproduced the decrease in thrust observed in the first few hundred hours of thruster operation and provided evidence to support the notion that low-energy ions (and not neutrals or electrons) are responsible for the majority of wall erosion. Recognizing the limitations of simple sputtering yield models employed by most authors, Yim et al. [87,88] utilized a molecular dynamics simulation to more accurately model sputtering, and Schinder et al. [90] constructed a three-dimensional surface mesh in an effort to recover observed sputtering-induced changes to the Hall thruster wall microstructure.

Further plasma discharge model fidelity was attained with the advent of particle-in-cell (PIC) models that solve the equations of motion for super particles representing groups of individual particles. Like fluid modelers, most authors [37,93–98] implementing PIC models for erosion calculation relied on simple theoretical fits of experimental data to determine sputtering yield. However, Cheng et al. [99] developed a variation of the Yamamura and Tawara model based on physical considerations, and Cao et al. [100] utilized the Huygens wavelet method to predict surface evolution.

Although the advent of predictive modeling will require more accurate experimental surface sputtering and near-wall plasma measurements, it will also require higher fidelity modeling approaches. Apart from the exceptions noted above, most efforts have applied increasingly mature plasma models to simple sputtering yield relations. Recovering sputtering-induced changes to surface microstructure and concomitant alterations to near-wall plasma properties will require the application of similarly sophisticated material models. Such an improvement would enable more accurate simulation of the coupled plasma–material sputtering mechanism.

5. Hall Thruster Erosion Reduction Concepts

Experimental and modeling efforts have shown that Hall thruster erosion rate increases with ion energy and ion flux to the wall. Attempts to reduce erosion have therefore centered on the development of Hall thruster variants that utilize different electric and magnetic field configurations to shield thruster walls from higher energy ions.

A prominent example, with origins that can be traced back to the 1960s, is the thruster with anode layer (TAL). This variant uses metallic walls, features a shorter discharge chamber, and employs metallic guard rings to provide a voltage bias that reduces electron wall losses. The bulk of the ionization and ion acceleration regions, where the most wall erosion occurs in an SPT, is pushed beyond the thruster exit plane. The TAL has extensive laboratory test and flight heritage in Russia but has not gained widespread acceptance as a flight thruster in the United States and Europe [3,101–103].

As noted above, the BPT-4000 extended life test reported an undetectably low wall erosion rate after 5600 h of operation [18]. Reduction in wall thickness caused by erosion early in thruster life changed the wall surface location relative to the magnetic field. This, in turn, altered the electric field near the wall and resulted in near-wall plasma conditions that more closely resembled those in the bulk of the discharge. The effect of this so-called "magnetic shielding" was to reduce the magnitude of the potential gradient in the sheath and to shift the electric field direction at the wall from pointing towards the wall to pointing along the wall [48,104–107]. The baseline technology of the BPT-4000 was licensed from Busek, and the BPT abbreviation represents "Busek-Primex Thruster." Aerojet Rocketdyne performed the qualification test that demonstrated low wall erosion, and NASA performed the extended lifetime test and much of the simulation and analysis work to provide theoretical basis for magnetic shielding.

Aerojet Rocketdyne captured the use of the low-erosion magnetic field topology in its Zero-Erosion™ Hall thruster line, and NASA utilized the concept to develop its own set of magnetically-shielded thrusters. The combined efforts of Aerojet Rocketdyne and NASA resulted in the 12.5 kW Hall Effect Rocket with Magnetic Shielding (HERMeS) that will serve as the Advanced Electric Propulsion System (AEPS) thruster for the Lunar Gateway in the Artemis program. Extensive qualification testing shows the expected lifetime of the thruster exceeds 50,000 h and that its

performance is comparable to that of a standard SPT [11]. Thruster life is expected to be limited by magnetic pole, rather than discharge chamber wall, erosion [108,109]. Figure 8 shows an image of the AEPS Engineering Test Unit 1.

Figure 8. Magnetically-shielded Advanced Electric Propulsion System (AEPS) Engineering Test Unit 1. Image reprinted with permission from [11], NASA, 2019.

Less technologically mature concepts include the cusped-field plasma thruster, the cylindrical Hall thruster, the wall-less Hall thruster, and the external discharge plasma thruster. These designs utilize unique magnetic field configurations to reduce ion flux to the wall. The cusped-field plasma thruster discharge chamber can be conical or cylindrical (as opposed to annular) and utilizes magnets in the chamber wall along the thruster axis to form magnetic cusps that limit electron diffusion to the anode [110]. The cylindrical Hall thruster features a cylindrical discharge chamber and places magnets near the thruster anode and in the thruster wall [111,112]. Removal of the inner wall in both the cusped-field plasma thruster and cylindrical Hall thruster causes these designs to have inherently lower wall surface-to-volume ratio compared to the SPT, which may explain their reduced wall erosion rates. The wall-less Hall thruster and external discharge plasma thruster utilize magnetic field configurations that push the discharge plasma away from thruster walls. The wall-less Hall thruster resembles an SPT, except that the anode is moved from the thruster base to the thruster exit plane. Ionization and ion acceleration occur outside the thruster exit plane [113,114]. The external discharge plasma thruster removes the SPT walls altogether and places magnets in the thruster baseplate [115]. The resulting electric and magnetic field configuration is similar to that generated by a circular planar magnetron [34].

Thruster erosion may also be reduced by substituting the BN or BN-SiO$_2$ in the SPT walls with a material of lower sputtering yield. Efforts have attempted to use diamond [116], BN-SiO$_2$ reinforced with SiA1ON [117], and BN reinforced with Al$_2$O$_3$-SiO$_2$ [118]. There is also interest in replacing the Hall thruster wall material with nanomaterials that could be engineered to have low sputter yield, self-healing properties, or even the capability to influence the thruster discharge in a way that shields the walls from ion impact [119]. The use of novel materials in thruster walls requires more development and testing.

6. Conclusions

Hall thruster erosion is a complex plasma-material interaction with important ramifications for device performance and life. Experimental work has measured wall erosion rate and demonstrated that erosion degrades thruster performance and ultimately ends thruster life. Detailed surface investigations have revealed the formation of anomalous erosion ridges, changes in surface composition, and microstructural surface feature development. Computational efforts have

successfully reproduced general erosion rate trends, but models are not yet predictive or capable of producing experimentally observed surface features.

More experimental work is required to accurately quantify the low ion energy sputtering rate of Hall thruster wall materials and to isolate the causes and impact of anomalous erosion ridges and microstructural surface features. It is known that erosion alters the wall surface, but more work is required to determine precisely how the material changes and what impact these changes have on the plasma. Though headway has been made in understanding the cause of exponentially decaying erosion rates and erosion-induced degradation of thruster performance, these topics are still not completely understood.

Predictive modeling of Hall thruster erosion is uniquely challenging and has not yet been achieved. Experimental uncertainties notwithstanding, predictive modeling requires an accurate representation of the coupled interaction between the plasma and the wall. High-fidelity plasma models have yet to be integrated with sophisticated material and sputtering models, so more effort is required in this area.

Finally, contemporary erosion mitigation concepts have yielded promising preliminary results. Magnetic shielding, in particular, may substantially increase thruster life without compromising performance. However, more work is required to flight-qualify low-erosion concepts and determine the efficacy of their low- and high-power variants.

References

1. Kim, V. Main physical features and processes determining the performance of stationary plasma thrusters. *J. Propul. Power* **1998**, *14*, 736–743, doi:10.2514/2.5335.
2. Zhurin, V.V.; Kaufman, H.R.; Robinson, R.S. Physics of closed drift thrusters. *Plasma Sources Sci. Technol.* **1999**, *8*, R1–R20, doi:10.1088/0963-0252/8/1/021.
3. Goebel, D.M.; Katz, I. Fundamentals of Electric Propulsion: Ion. and Hall Thrusters; John Wiley & Sons: Hoboken, NJ, USA, 2008; pp. 1–446.
4. Charles, C. Plasmas for spacecraft propulsion. *J. Phys. D* **2009**, *42*, 163001, doi:10.1088/0022-3727/42/16/163001.
5. Ahedo, E. Plasmas for space propulsion. *Plasma Phys. Control. Fusion* **2011**, *53*, 124037, doi:10.1088/0741-3335/53/12/124037.
6. Mazouffre, S. Electric propulsion for satellites and spacecraft: Established technologies and novel approaches. *Plasma Sources Sci. Technol.* **2016**, *25*, 033002, doi:10.1088/0963-0252/25/3/033002.
7. Boeuf, J.-P. Tutorial: Physics and modeling of Hall thrusters. *J. Appl. Phys.* **2017**, *121*, 011101, doi:10.1063/1.4972269.
8. Hara, K. An overview of discharge plasma modeling for Hall effect thrusters. *Plasma Sources Sci. Technol.* **2019**, *28*, 044001, doi:10.1088/1361-6595/ab0f70.
9. Lev, D.; Myers, R.M.; Lemmer, K.M.; Kolbeck, J.; Koizumi, H.; Polzin, K. The technological and commercial expansion of electric propulsion. *Acta Astronaut.* **2019**, *159*, 213–227, doi:10.1016/j.actaastro.2019.03.058.

10. Oh, D.Y.; Collins, S.; Drain, T.; Hart, W.; Imken, T.; Larson, K.; Marsh, D.; Muthulingam, D.; Snyder, J.S.; Trofimov, D.; et al. Development of the Psyche Mission for NASA's Discovery Program. In *Proceedings of the 36th International Electric Propulsion Conference, Vienna, Austria, 15–20 September 2019*; Electric Rocket Propulsion Society: Brook Park, OH, USA, 2019; IEPC Paper 2019-192.

11. Hofer, R.; Lobbia, R.; Chaplin, V.; Ortega, A.; Mikellides, I.; Polk, J.; Kamhawi, H.; Frieman, J.; Huang, W.; Peterson, P.; et al. Completing the Development of the 12.5 kW Hall Effect Rocket with Magnetic Shielding (HERMeS). In *Proceedings of the 36th International Electric Propulsion Conference, Vienna, Austria, 15–20 September 2019*; Electric Rocket Propulsion Society: Brook Park, OH, USA, 2019; IEPC Paper 2019-193.

12. Maslennikov, N.A. Lifetime of the Stationary Plasma Thruster. In *Proceedings of the 24th International Electric Propulsion Conference, Moscow, Russia, 19–23 September 1995*; Electric Rocket Propulsion Society: Brook Park, OH, USA, 1995; IEPC Paper 1995-075.

13. Mazouffre, S.; Dubois, F.; Albarede, L.; Pagnon, D.; Touzeau, M.; Dudeck, M. Plasma induced erosion phenomena in a Hall thruster. In *Proceedings of the the International Conference on the Recent Advances in Space Technologies, Istanbul, Turkey, 20–22 November 2003*; Institute of Electrical and Electronics Engineers: Piscataway, NJ, USA, 2003; pp. 69–74.

14. Arhipov, B.A.; Bober, A.S.; Gnizdor, R.Y.; Kozubsky, K.N.; Korakin, A.I.; Maslennikov, N.A.; Pridannikov, S.Y. The Results of 7000-Hour SPT-100 Life Testing. In *Proceedings of the 24th International Electric Propulsion Conference, Moscow, Russia, 19–23 September 1995*; Electric Rocket Propulsion Society: Brook Park, OH, USA, 1995; IEPC Paper 1995-39.

15. Garner, C.; Brophy, J.; Polk, J.; Pless, L. A 5,730-hr cyclic endurance test of the SPT-100. In *Proceedings of the 31st Joint Propulsion Conference and Exhibit, San Diego, CA, USA, 10–12 July 1995*; American Institute of Aeronautics and Astronautics: Reston, VA, USA, 1995; AIAA Paper 1995-2667, doi:10.2514/6.1995-2667.

16. Lyszyk, M.; Klinger, E.; Secheresse, O.; Bugeat, J.; Valentian, D.; Cadiou, A.; Beltan, T.; Gelas, C. Qualification status of the PPS 1350 plasma thruster. In *Proceedings of the 35th Joint Propulsion Conference and Exhibit, Los Angeles, CA, USA 20–24 June 1999*; American Institute of Aeronautics and Astronautics: Reston, VA, USA, 1999; AIAA Paper 1999-2278, doi:10.2514/6.1999-2278.

17. Marchandise, F.R.; Biron, J.; Gambon, M.; Cornu, N.; Damon, F.; Estublier, D. The PPS-1350 qualification demonstration 7500h on ground, about 5000h in flight. In *Proceedings of the 29th International Electric Propulsion Conference, Princeton, NJ, USA, 31 October – 4 November 2005*; Electric Rocket Propulsion Society: Brook Park, OH, USA, 2005; IEPC Paper 2005-209.

18. de Grys, K.; Mathers, A.; Welander, B.; Khayms, V. Demonstration of 10,400 Hours of Operation on 4.5 kW Qualification Model Hall Thruster. In *Proceedings of the 46th AIAA/ASME/SAE/ASEE Joint Propulsion Conference & Exhibit, Nashville, TN, USA, 25–28 July 2010*; American Institute of Aeronautics and Astronautics: Reston, VA, USA, 2010; AIAA Paper 2010-6698, doi:10.2514/6.2010-6698.

19. Shagaida, A.A.; Gorshkov, O.A.; Tomilin, D.A. Influence of the erosion of the discharge channel wall on the efficiency of a stationary plasma thruster. *Tech. Phys.* **2012**, *57*, 1083–1089, doi:10.1134/s1063784212080221.

20. Zurbach, S.; Duchemin, O.B.; Vial, V.; Marchandise, F.; Cornu, N.; Arcis, N. Qualification of the PPS-1350 Hall plasma thruster at 2.5 kW. In *Proceedings of the 49th AIAA/ASME/SAE/ASEE Joint Propulsion Conference, San Jose, CA, USA, 14-17 July 2013*; American Institute of Aeronautics and Astronautics: Reston, VA, USA, 2013; AIAA Paper 2013-4113, doi:10.2514/6.2013-4113.

21. Choueiri, E.Y. Plasma oscillations in Hall thrusters. *Phys. Plasmas* **2001**, *8*, 1411–1426, doi:10.1063/1.1354644.

22. Zidar, D.G.; Rovey, J.L. Hall-Effect Thruster Channel Surface Properties Investigation. *J. Propul. Power* **2012**, *28*, 334–343, doi:10.2514/1.B34312.

23. Burton, T.; Schinder, A.M.; Capuano, G.; Rimoli, J.J.; Walker, M.L.R.; Thompson, G.B. Plasma-Induced Erosion on Ceramic Wall Structures in Hall-Effect Thrusters. *J. Propul. Power* **2014**, *30*, 690–695, doi:10.2514/1.B34882.

24. Langendorf, S. Effects of Electron Emission on Plasma Sheaths. Ph.D. Thesis, Georgia Institute of Technology, Atlanta, GA, USA, 2015.

25. Siddiqui, M.U.; Thompson, D.S.; Jackson, C.D.; Kim, J.F.; Hershkowitz, N.; Scime, E.E. Models, assumptions, and experimental tests of flows near boundaries in magnetized plasmas. *Phys. Plasmas* **2016**, *23*, 057101, doi:10.1063/1.4943523.

26. Gascon, N.; Dudeck, M.; Barral, S. Wall material effects in stationary plasma thrusters. I. Parametric studies of an SPT-100. *Phys. Plasmas* **2003**, *10*, 4123–4136, doi:10.1063/1.1611880.

27.	Barral, S.; Makowski, K.; Peradzyński, Z.; Gascon, N.; Dudeck, M. Wall material effects in stationary plasma thrusters. II. Near-wall and in-wall conductivity. *Phys. Plasmas* **2003**, *10*, 4137–4152, doi:10.1063/1.1611881.

28.	Schinder, A.M. Investigation of Hall Effect Thruster Channel Wall Erosion Mechanisms. Ph.D. Thesis, Georgia Institute of Technology, Atlanta, GA, USA, 2016.

29.	Lipp, A.; Schwetz, K.A.; Hunold, K. Hexagonal Boron Nitride: Fabrication, Properties and Applications. *J. Eur. Ceram. Soc.* **1989**, *5*, 3–9, doi:10.1016/0955-2219(89)90003-4.

30.	Naftaly, M.; Leist, J. Investigation of optical and structural properties of ceramic boron nitride by terahertz time-domain spectroscopy. *Appl. Opt.* **2013**, *52*, B20–B25, doi:10.1364/AO.52.000B20.

31.	Duan, X.; Yang, Z.; Chen, L.; Tian, Z.; Cai, D.; Wang, Y.; Jia, D.; Zhou, Y. Review on the properties of hexagonal boron nitride matrix composite ceramics. *J. Eur. Ceram. Soc.* **2016**, *36*, 3725–3737, doi:10.1016/j.jeurceramsoc.2016.05.007.

32.	Smentkowski, V.S. Trends in sputtering. *Prog. Surf. Sci.* **2000**, *64*, 1–58, doi:10.1016/S0079-6816(99)00021-0.

33.	Murty, M.V.R. Sputtering: The material erosion tool. *Surf. Sci.* **2002**, *500*, 523–544, doi:10.1016/s0039-6028(01)01586-2.

34.	Abolmasov, S.N. Physics and engineering of crossed-field discharge devices. *Plasma Sources Sci. Technol.* **2012**, *21*, 035006, doi:10.1088/0963-0252/21/3/035006.

35.	Rubin, B.; Topper, J.L.; Yalin, A.P. Total and differential sputter yields of boron nitride measured by quartz crystal microbalance. *J. Phys. D* **2009**, *42*, 205205, doi:10.1088/0022-3727/42/20/205205.

36.	Huang, W.S.; Gallimore, A.D.; Smith, T.B. Interior and Near-Wall Ion Velocity Distribution Functions in the H6 Hall Thruster. *J. Propul. Power* **2013**, *29*, 1146–1154, doi:10.2514/1.B34712.

37.	Sommier, E.; Scharfe, M.K.; Gascon, N.; Cappelli, M.A.; Fernandez, E. Simulating Plasma-Induced Hall Thruster Wall Erosion With a Two-Dimensional Hybrid Model. *IEEE Trans. Plasma Sci.* **2007**, *35*, 1379–1387, doi:10.1109/tps.2007.905943.

38.	Garnier, Y.; Viel, V.; Rousell, J.-F. Investigation of Xenon Ion Sputtering of One Ceramic Material Used in SPT Discharge Chamber. In *Proceedings of the 26th International Electric Propulsion Conference, Kitakyushu, Japan, 17–21 October 1999*; Electric Rocket Propulsion Society: Brook Park, OH, USA, 1999; IEPC Paper 1999-83.

39.	Garnier, Y.; Viel, V.; Roussel, J.-F.; Bernard, J. Low-energy xenon ion sputtering of ceramics investigated for stationary plasma thrusters. *J. Vac. Sci. Technol. A.* **1999**, *17*, 3246–3254, doi:10.1116/1.582050.

40.	Ranjan, M.; Sharma, A.; Vaid, A.; Bhatt, T.; Nandalan, V.; James, M.G.; Revathi, H.; Mukherjee, S. BN/BNSiO2 sputtering yield shape profiles under stationary plasma thruster operating conditions. *Aip Adv.* **2016**, *6*, 095224, doi:10.1063/1.4964312.

41.	Brault, P. Multiscale Molecular Dynamics Simulation of Plasma Processing: Application to Plasma Sputtering. *Front. Phys.* **2018**, *6*, doi:10.3389/fphy.2018.00059.

42.	Brown, N.P.; Whittaker, C.B.; Rimoli, J.J.; Ready, W.J.; Walker, M.L.R. Formation and Impact of Microcracks in Plasma Erosion of M26 Boron Nitride. *J. Propul. Power* **2020**, Accepted.

43.	Langendorf, S.; Walker, M. Effect of secondary electron emission on the plasma sheath. *Phys. Plasmas* **2015**, *22*, 033515, doi:10.1063/1.4914854.

44.	Kahn, J.; Zhurin, V.V.; Kozubsky, K.; Randolph, T.; Kim, V. Effect of Background Nitrogen and Oxygen on Insulator Erosion in the SPT-100. In *Proceedings of the 23rd International Electric Propulsion Conference, Seattle, WA, USA, 13–16 September 1993*; Electric Rocket Propulsion Society: Brook Park, OH, USA, 1993; IEPC Paper 1993-093.

45.	Petrosov, V.A.; Vasin, A.I.; Baranov, V.I.; Wetch, J.R.; Britt, E.J.; Wong, S.P.; Lin, R. A 2000 Hours Lifetime Test Results of 1.3 kW T-100 Electric Thruster. In *Proceedings of the 24th International Electric Propulsion Conference, Moscow, Russia, 19–23 September 1995*; Electric Rocket Propulsion Society: Brook Park, OH, USA, 1995; IEPC Paper 1995-041.

46.	Mason, L.; Jankovsky, R.; Manzella, D. 1000 hours of testing on a 10 kilowatt Hall effect thruster. In *Proceedings of the 37th Joint Propulsion Conference and Exhibit, Salt Lake City, UT, USA, 8–11 July 2001*; American Institute of Aeronautics and Astronautics: Reston, VA, USA, 2001; AIAA Paper 2001-3773, doi:10.2514/6.2001-3773.

47.	Peterson, P.; Jacobson, D.; Manzella, D.; John, J. The Performance and Wear Characterization of a High-Power High-Isp NASA Hall Thruster. In *Proceedings of the 41st AIAA/ASME/SAE/ASEE Joint Propulsion Conference & Exhibit, Tucson, AZ, USA, 10–13 July 2005*; American Institute of Aeronautics and Astronautics: Reston, VA, USA, 2005; AIAA Paper 2005-4243, doi:10.2514/6.2005-4243.

48. Mikellides, I.; Katz, I.; Hofer, R.; Goebel, D.; de Grys, K.; Mathers, A. Magnetic Shielding of the Acceleration Channel Walls in a Long-Life Hall Thruster. In *Proceedings of the 46th AIAA/ASME/SAE/ASEE Joint Propulsion Conference & Exhibit, Nashville, TN, USA, 25–28 July 2010*; American Institute of Aeronautics and Astronautics: Reston, VA, USA, 2010; AIAA Paper 2010-6942, doi:10.2514/6.2010-6942.

49. Andreussi, T.; Saravia, M.M.; Ferrato, E.; Piragino, A.; Rossodivita, A.; Andrenucci, M. Identification, Evaluation and Testing of Alternative Propellants for Hall Effect Thrusters. In *Proceedings of the 35th International Electric Propulsion Conference, Atlanta, GA, USA, 8–12 October 2017; Electric Rocket* Propulsion Society: Brook Park, OH, USA, 2017; IEPC Paper 2017-380.

50. Nakles, M.R.; Hargus, W.A.; Delgado, J.J.; Corey, R.L. A 205 Hour Krypton Propellant Life Test of the SPT-100 Operating at 2 kW. In *Proceedings of the 33rd International Electric Propulsion Conference, Washington, DC, USA, 7–10 October 2013*; Electric Rocket Propulsion Society: Brook Park, OH, USA, 2013; IEPC Paper 2013-347.

51. Peterson, P.; Manzella, D.; Jacobson, D. Investigation of the Erosion Characteristics of a Laboratory Hall Thruster. In *Proceedings of the 39th AIAA/ASME/SAE/ASEE Joint Propulsion Conference and Exhibit, Huntsville, AL, USA, 20–23 July 2003*; American Institute of Aeronautics and Astronautics: Reston, VA, USA, 2003; AIAA Paper 2003-5005, doi:10.2514/6.2003-5005.

52. Bugrova, A.I.; Bishaev, A.M.; Desyatskov, A.V.; Kozintseva, M.V.; Prioul, M. Spectral Investigation of SPT MAG Insulator Erosion. In *Proceedings of the 29th International Electric Propulsion Conference, Princeton, NJ, USA, 31 October – 4 November 2005*; Electric Rocket Propulsion Society: Brook Park, OH, USA, 2005; IEPC Paper 2005-167.

53. Zhang, Z.; Ren, J.X.; Tang, H.B.; Cao, J.B.; Cao, S.; Chen, Z.Y.; Ling, W.Y.L.; Zhao, R.K. The facility effects of a Hall effect thruster's relative exhaust direction in ground tests. *Vacuum* **2018**, *155*, 199–209, doi:10.1016/j.vacuum.2018.06.004.

54. Ortega, A.L.; Mikellides, I.G.; Chaplin, V.H.; Snyder, J.S.; Lenguito, G. Facility pressure effects on a Hall thruster with an external cathode: I. Numerical simulations. *Plasma Sources Sci. Technol.* **2020**, *29*, 035011, doi:10.1088/1361-6595/ab6c7e.

55. Misuri, T.; Milani, A.; Andrenucci, M. Development of a Telemicroscopy Diagnostic Apparatus and Erosion Modelling in Hall Effect Thrusters. In *Proceedings of the 31st International Electric Propulsion Conference, Ann Arbor, MI, USA, 20–24 September 2009*; Electric Rocket Propulsion Society: Brook Park, OH, USA, 2009; IEPC Paper 2009-036.

56. Andreussi, T.; Pieri, L.; Albertoni, R.; Andrenucci, M.; Duchemin, O. Telemicroscopy Erosion Measurements of 5 kW-Class Hall Effect Thruster Channel Walls. In *Proceedings of the 34th International Electric Propulsion Conference, Hyogo-Kobe, Japan, 7–10 July 2015*; Electric Rocket Propulsion Society: Brook Park, OH, USA, 2015; IEPC Paper 2015-348.

57. Tao, L.; Lee, B.; Yalin, A.; Yamamoto, N.; Gallimore, A. Development of a Cavity Ring-Down Spectroscopy Sensor for Boron Nitride Erosion in Hall Thrusters. In *Proceedings of the 31st International Electric Propulsion Conference, Ann Arbor, MI, USA, 20–24 September 2009*; Electric Rocket Propulsion Society: Brook Park, OH, USA, 2009; IEPC Paper 2009-146.

58. Yamamoto, N.; Tao, L.; Rubin, B.; Williams, J.D.; Yalin, A.P. Sputter Erosion Sensor for Anode Layer-Type Hall Thrusters Using Cavity Ring-Down Spectroscopy. *J. Propul. Power* **2010**, *26*, 142–148, doi:10.2514/1.44784.

59. Celik, M.; Batishchev, O.; Martinez-Sanchez, M. Use of emission spectroscopy for real-time assessment of relative wall erosion rate of BHT-200 hall thruster for various regimes of operation. *Vacuum* **2010**, *84*, 1085–1091, doi:10.1016/j.vacuum.2010.01.031.

60. Shmelev, A.V.; Lovtsov, A.S. Investigation of Discharge Power Influence on Erosion Rate of SPT Discharge Chamber using Spectroscopic Method. In *Proceedings of the 32nd International Electric Propulsion Conference, Wiesbaden, Germany, 11–15 September 2011*; Electric Rocket Propulsion Society: Brook Park, OH, USA, 2011; IEPC Paper 2011-024.

61. Shmelev, A.V.; Lovtsov, A.S. The Effect of Magnetic Field Configuration and Propellant Supply Rate on Insulator Erosion in a Hall Thruster. *Tech. Phys. Lett.* **2012**, *38*, 544–547, doi:10.1134/s1063785012060168.

62. Balika, L.; Focsa, C.; Gurlui, S.; Pellerin, S.; Pellerin, N.; Pagnon, D.; Dudeck, M. Laser-induced breakdown spectroscopy in a running Hall Effect Thruster for space propulsion. *Spectrochim. Acta B* **2012**, *74-75*, 184–189, doi:10.1016/j.sab.2012.06.030.

63. Lee, B.C.; Huang, W.; Tao, L.; Yamamoto, N.; Gallimore, A.D.; Yalin, A.P. A cavity ring-down spectroscopy sensor for real-time Hall thruster erosion measurements. *Rev. Sci. Instrum.* **2014**, *85*, 053111, doi:10.1063/1.4879135.

64. Dragnea, H.C.; Boyd, I.D.; Lee, B.C.; Yalin, A.P. Characterization of Eroded Boron Atoms in the Plume of a Hall Thruster. *IEEE Trans. Plasma Sci.* **2015**, *43*, 35–44, doi:10.1109/TPS.2014.2320851.

65. Arhipov, B.A.; Gnizdor, R.Y.; Maslennikov, N.A.; Morozov, A.I. Anomalous erosion of an insulator under the action of a stream of plasma. *Sov. J. Plasma Phys.* **1992**, *18*, 641–643.

66. Laurent, B.; Rossi, A.; Öberg, M.; Zurbach, S.; Largeau, G.; Lasgorceix, P.; Estublier, D.; Boniface, C. High Throughput 1.5 kW Hall Thruster for Satcoms. In *Proceedings of the 36th International Electric Propulsion Conference, Vienna, Austria, 15–20 September 2019*; Electric Rocket Propulsion Society: Brook Park, OH, USA, 2019; IEPC Paper 2019-274.

67. Morozov, A.I.; Savelyev, V.V. The Electron Dynamics in SPT-Channel and the Problem of Anomalous Erosion. In *Proceedings of the 24th International Electric Propulsion Conference, Moscow, Russia, 19–23 September 1995*; Electric Rocket Propulsion Society: Brook Park, OH, USA, 1995; IEPC Paper 1995-042.

68. Baranov, V.I.; Nazarenko, Y.S.; Petrosov, V.A.; Vasin, A.I.; Yashnov, Y.M. The Mechanism of Anomalous Erosion in Accelerators with Closed Drift Electrons. In *Proceedings of the 24th International Electric Propulsion Conference, Moscow, Russia, 19–23 September 1995*; Electric Rocket Propulsion Society: Brook Park, OH, USA, 1995; IEPC Paper 1995-043.

69. Schinder, A.M.; Rimoli, J.J.; Walker, M.L.R. Investigation of Plasma Material Erosion Under Mechanical Stress. *J. Propul. Power* **2016**, *33*, 433–447, doi:10.2514/1.B36253.

70. Manzella, D.; Yim, J.; Boyd, I. Predicting Hall Thruster Operational Lifetime. In *Proceedings of the 40th AIAA/ASME/SAE/ASEE Joint Propulsion Conference and Exhibit, Fort Lauderdale, FL, USA, 11–14 July 2004*; American Institute of Aeronautics and Astronautics: Reston, VA, USA, 2004; AIAA Paper 2004-3953, doi:10.2514/6.2004-3953.

71. Yu, D.R.; Li, Y.Q. Volumetric erosion rate reduction of Hall thruster channel wall during ion sputtering process. *J. Phys. D* **2007**, *40*, 2526–2532, doi:10.1088/0022-3727/40/8/017.

72. Dorf, L.; Raitses, Y.; Fisch, N.J.; Semenov, V. Effect of anode dielectric coating on Hall thruster operation. *Appl. Phys. Lett.* **2004**, *84*, 1070–1072, doi:10.1063/1.1646727.

73. Cao, X.F.; Hang, G.R.; Liu, H.; Meng, Y.C.; Luo, X.M.; Yu, D.R. Hybrid-PIC simulation of sputtering product distribution in a Hall thruster. *Plasma Sci. Technol.* **2017**, *19*, 105501, doi:10.1088/2058-6272/aa7940.

74. Malik, H.K.; Tyagi, J.; Sharma, D. Growth of Rayleigh instability in a Hall thruster channel having dust in exit region. *Aip Adv.* **2019**, *9*, 055220, doi:10.1063/1.5050688.

75. Duan, X.; Ding, Y.; Jia, D.; Jing, N.; Yang, Z.; He, P.; Tian, Z.; Wang, S.; Wang, Y.; Zhou, Y.; et al. Ion sputtering erosion mechanisms of h-BN composite ceramics with textured microstructures. *J. Alloy. Compd.* **2014**, *613*, 1–7, doi:10.1016/j.jallcom.2014.05.221.

76. Satonik, A.J.; Rovey, J.L.; Hilmas, G. Effects of Plasma Exposure on Boron Nitride Ceramic Insulators for Hall-Effect Thrusters. *J. Propul. Power* **2014**, *30*, 656–663, doi:10.2514/1.B34877.

77. Sarrailh, P.; Belhaj, M.; Inguimbert, V.; Boniface, C. Synergic erosion of ceramic by electron and ion simultaneous irradiation of the Hall thruster channel walls. In *Proceedings of the 35th International Electric Propulsion Conference, Atlanta, GA, USA, 8–12 October 2017*; Electric Rocket Propulsion Society: Brook Park, OH, USA, 2017; IEPC Paper 2017-314.

78. Kim, V.; Kozlov, V.; Semenov, A.; Shkarban, I. Investigation of the Boron Nitride based Ceramics Sputtering Yield Under its Bombardment by Xe and Kr ions. In *Proceedings of the 27th International Electric Propulsion Conference, Pasadena, CA, USA, 15–19 October 2001*; Electric Rocket Propulsion Society: Brook Park, OH, USA, 2001; IEPC Paper 2001-73.

79. Baranov, V.I.; Vasin, A.I.; Kalyaev, A.A.; Petrosov, V.A. Prediction of Electric Thruster Lifetime. In *Proceedings of the 23rd International Electric Propulsion Conference, Seattle, WA, USA, 13–16 September 1993*; Electric Rocket Propulsion Society: Brook Park, OH, USA, 1993; IEPC Paper 1993-099.

80. Kalyaev, A.A.; Petrosov, V.A.; Baranov, V.I. Stationary Plasma Hall Thruster Lifetime Prediction. In *Proceedings of the 24th International Electric Propulsion Conference, Moscow, Russia, 19–23 September 1995*; Electric Rocket Propulsion Society: Brook Park, OH, USA, 1995; IEPC Paper 1995-057.

81. Bhat, S.; Mishra, A. Prediction of liner erosion and life estimation of Stationary Plasma Thrusters using Machine Learning. In *Proceedings of the 36th International Electric Propulsion Conference, Vienna, Austria, 15–20 September 2019*; Electric Rocket Propulsion Society: Brook Park, OH, USA, 2019; IEPC Paper 2019-749.

82. Komurasaki, K.; Arakawa, Y. Performance calculation of Hall thrusters. *Acta Astronaut.* **1996**, *38*, 185–192, doi:10.1016/0094-5765(96)00008-2.

83. Clauss, C.; Day, M.; Kim, V.; Kondakov, Y.; Randolph, T. Preliminary study of possibility to ensure large enough lifetime of SPT operating under increased powers. In *Proceedings of the 33rd Joint Propulsion Conference and Exhibit, Seattle, WA, USA, 6–9 July 1997*; American Institute of Aeronautics and Astronautics: Reston, VA, USA, 1997; AIAA Paper 1997-2789, doi:10.2514/6.1997-2789.

84. Roy, S.; Pandey, B.P. Plasma-wall interaction inside a Hall thruster. *J. Plasma Phys.* **2002**, *68*, 305–319, doi:10.1017/s0022377802002027.

85. Garrigues, L.; Hagelaar, G.J.M.; Bareilles, J.; Boniface, C.; Boeuf, J.P. Model study of the influence of the magnetic field configuration on the performance and lifetime of a Hall thruster. *Phys. Plasmas* **2003**, *10*, 4886–4892, doi:10.1063/1.1622670.

86. Gamero-Castaño, M.; Katz, I. Estimation of Hall Thruster Erosion Using HPHall. In *Proceedings of the 29th International Electric Propulsion Conference, Princeton, NJ, USA, 31 October – 4 November 2005*; Electric Rocket Propulsion Society: Brook Park, OH, USA, 2005; IEPC Paper 2005-303.

87. Yim, J.T.; Boyd, I.D.; Keidar, M. Hall Thruster Erosion Prediction Using A Hydrodynamic Plasma Model And Sputtering Simulation. In *Proceedings of the 30th International Electric Propulsion Conference, Florence, Italy, 17–20 September 2007*; Electric Rocket Propulsion Society: Brook Park, OH, USA, 2007; IEPC Paper 2007-034.

88. Yim, J.T.; Falk, M.L.; Boyd, I.D. Modeling low energy sputtering of hexagonal boron nitride by xenon ions. *J. Appl. Phys.* **2008**, *104*, 123507, doi:10.1063/1.2987090.

89. Oghienko, S.A.; Saleh, H.D.; Khitko, A.V.; Kulagin, S.N.; Petrenko, A.N. Two Approaches to the Studying of a Hall Thruster Discharge Chamber Erosion Process. In *Proceedings of the 31st International Electric Propulsion Conference, Ann Arbor, MI, USA, 20–24 September 2009*; Electric Rocket Propulsion Society: Brook Park, OH, USA, 2009; IEPC Paper 2009-037.

90. Schinder, A.M.; Walker, M.; Rimoli, J.J. Three-Dimensional Model for Erosion of a Hall-Effect Thruster Discharge Channel Wall. *J. Propul. Power* **2014**, *30*, 1373–1382, doi:10.2514/1.B35098.

91. Mikellides, I.G.; Ortega, A.L. 2D (r-z) numerical simulations of the plasma and channel erosion in a 100kW class nested Hall thruster. *Plasma Sources Sci. Technol.* **2018**, *27*, 075001, doi:10.1088/1361-6595/aacacb.

92. Yamamura, Y.; Tawara, H. Energy dependence of ion-induced sputtering yields from monatomic solids at normal incidence. *Data Nucl. Data Tables* **1996**, *62*, 149–253, doi:10.1006/adnd.1996.0005.

93. Ahedo, E.; Antón, A.; Garmendia, I.; Caro, I.; González del Amo, J. Simulation of wall erosion in Hall thrusters. In *Proceedings of the 30th International Electric Propulsion Conference, Florence, Italy, 17–20 September 2007*; Electric Rocket Propulsion Society: Brook Park, OH, USA, 2007; IEPC Paper 2007-067.

94. Hofer, R.R.; Mikellides, I.G.; Katz, I.; Goebel, D.M. BPT-4000 Hall Thruster Discharge Chamber Erosion Model Comparison with Qualification Life Test Data. In *Proceedings of the 30th International Electric Propulsion Conference, Florence, Italy, 17–20 September 2007*; Electric Rocket Propulsion Society: Brook Park, OH, USA, 2007; IEPC Paper 2007-267.

95. Koizumi, H.; Komurasaki, K.; Arakawa, Y. Numerical prediction of wall erosion on a Hall thruster. *Vacuum* **2008**, *83*, 67–71, doi:10.1016/j.vacuum.2008.03.096.

96. Garrigues, L.; Boniface, C.; Hagelaar, G.J.M.; Boeut, J.P.; Duchemin, O. Performance Modeling of a Thrust Vectoring Device for Hall Effect Thrusters. *J. Propul. Power* **2009**, *25*, 1003–1012, doi:10.2514/1.39680.

97. Yan, L.; Wang, P.Y.; Ou, Y.H.; Kang, X.L. Numerical Study of Hall Thruster Plume and Sputtering Erosion. *J. Appl. Math.* **2012**, 10.1155/2012/327021, 327021, doi:10.1155/2012/327021.

98. Liu, J.W.; Li, H.; Hu, Y.L.; Liu, X.Y.; Ding, Y.J.; Wei, L.Q.; Yu, D.R.; Wang, X.G. Particle-in-cell simulation of the effect of curved magnetic field on wall bombardment and erosion in a hall thruster. *Contrib. Plasma Phys.* **2019**, *59*, e201800001, doi:10.1002/ctpp.201800001.

99. Cheng, S.; Martinez-Sanchez, M. Hybrid Particle-in-Cell Erosion Modeling of Two Hall Thrusters. *J. Propul. Power* **2008**, *24*, 987–998, doi:10.2514/1.36179.

100. Cao, H.J.; Cao, Y.; Chu, Y.C.; He, X.M.; Lin, T. A Huygens immersed-finite-element particle-in-cell method for modeling plasma-surface interactions with moving interface. *Commun. Nonlinear Sci. Numer. Simul.* **2018**, *59*, 132–148, doi:10.1016/j.cnsns.2017.10.015.

101. Garner, C.; Brophy, J.; Polk, J.; Semenkin, S.; Garkusha, V.; Tverdokhlebov, S.; Marrese, C. Experimental Evaluation of Russian Anode Layer Thrusters. In *Proceedings of the 30th Joint Propulsion Conference and Exhibit, Indianapolis, IN, USA, 27–29 June 1994*; American Institute of Aeronautics and Astronautics: Reston, VA, USA, 1994; AIAA Paper 94-3010, doi:10.2514/6.1994-3010.

102. Semenkin, A.; Kochergin, A.; Rusakov, A.; Bulaev, V.; Yuen, J.; Shoji, J.; Garner, C.; Manzella, D. Development program and preliminary test results of the TAL-110 thruster. In *Proceedings of the 35th Joint Propulsion Conference and Exhibit, Los Angeles, CA, USA, 20–24 June 1999*; American Institute of Aeronautics and Astronautics: Reston, VA, USA, 1999; AIAA Paper 99-2279, doi:10.2514/6.1999-2279.

103. Solodukhin, A.E.; Semenkin, A.V. Study of Discharge Channel Erosion in Multi Mode Anode Layer Thruster. In *Proceedings of the 28th International Electric Propulsion Conference, Toulouse, France, 17-21 March 2003*; Electric Rocket Propulsion Society: Brook Park, OH, USA, 2003; IEPC Paper 2003-0204.

104. Mikellides, I.G.; Katz, I.; Hofer, R.R.; Goebel, D.M. Magnetic shielding of a laboratory Hall thruster. I. Theory and validation. *J. Appl. Phys.* **2014**, *115*, 043303, doi:10.1063/1.4862313.

105. Mikellides, I.G.; Katz, I.; Hofer, R.R.; Goebel, D.M. Magnetic shielding of walls from the unmagnetized ion beam in a Hall thruster. *Appl. Phys. Lett.* **2013**, *102*, 023509, doi:10.1063/1.4776192.

106. Mikellides, I.G.; Katz, I.; Hofer, R.R.; Goebel, D.M.; de Grys, K.; Mathers, A. Magnetic shielding of the channel walls in a Hall plasma accelerator. *Phys. Plasmas* **2011**, *18*, 033501, doi:10.1063/1.3551583.

107. Hofer, R.R.; Goebel, D.M.; Mikellides, I.G.; Katz, I. Magnetic shielding of a laboratory Hall thruster. II. Experiments. *J. Appl. Phys.* **2014**, *115*, 043304, doi:10.1063/1.4862314.

108. Ding, Y.J.; Wang, L.; Fan, H.T.; Li, H.; Xu, W.F.; Wei, L.Q.; Li, P.; Yu, D.R. Simulation research on magnetic pole erosion of Hall thrusters. *Phys. Plasmas* **2019**, *26*, 023520, doi:10.1063/1.5077041.

109. Ortega, A.L.; Mikellides, I.G.; Sekerak, M.J.; Jorns, B.A. Plasma simulations in 2-D (r-z) geometry for the assessment of pole erosion in a magnetically shielded Hall thruster. *J. Appl. Phys.* **2019**, *125*, 033302, doi:10.1063/1.5077097.

110. Gildea, S.R.; Matlock, T.S.; Martinez-Sanchez, M.; Hargus, W.A. Erosion Measurements in a Low-Power Cusped-Field Plasma Thruster. *J. Propul. Power* **2013**, *29*, 906–918, doi:10.2514/1.B34607.

111. Smirnov, A.; Raitses, Y.; Fisch, N.J. Plasma measurements in a 100 W cylindrical Hall thruster. *J. Appl. Phys.* **2004**, *95*, 2283–2292, doi:10.1063/1.1642734.

112. Smirnov, A.; Raitses, Y.; Fisch, N. Performance Studies of Miniaturized Cylindrical and Annular Hall Thrusters. In *Proceedings of the 38th AIAA/ASME/SAE/ASEE Joint Propulsion Conference & Exhibit, Indianapolis, IN, USA, 27–29 June 1994*; American Institute of Aeronautics and Astronautics: Reston, VA, USA, 2002; AIAA Paper 2002-3823, doi:10.2514/6.2002-3823.

113. Mazouffre, S.; Tsikata, S.; Vaudolon, J. Development and experimental characterization of a wall-less Hall thruster. *J. Appl. Phys.* **2014**, *116*, 243302, doi:10.1063/1.4904965.

114. Ding, Y.J.; Peng, W.J.; Sun, H.Z.; Wei, L.Q.; Zeng, M.; Wang, F.F.; Yu, D.R. Performance characteristics of No-Wall-Losses Hall Thruster. *Eur. Phys. J. Spec. Top.* **2017**, *226*, 2945–2953, doi:10.1140/epjst/e2016-60247-y.

115. Karadag, B.; Cho, S.; Funaki, I. Thrust performance, propellant ionization, and thruster erosion of an external discharge plasma thruster. *J. Appl. Phys.* **2018**, *123*, 153302, doi:10.1063/1.5023829.

116. Meezan, N.B.; Gascon, N.; Cappelli, M.A. Linear Geometry Hall Thruster with Boron Nitride and Diamond Walls. In *Proceedings of the 27th International Electric Propulsion Conference, Pasadena, CA, USA, 15–19 October 2001*; Electric Rocket Propulsion Society: Brook Park, OH, USA, 2001; IEPC Paper 2001-039.

117. Tian, Z.; Duan, X.M.; Yang, Z.H.; Ye, S.Q.; Jia, D.C.; Zhou, Y. Microstructure and Erosion Resistance of in-situ SiAlON Reinforced BN-SiO2 Composite Ceramics. *J. Wuhan Univ. Technol.-Mat. Sci. Ed.* **2016**, *31*, 315–320, doi:10.1007/s11595-016-1369-9.

118. Duan, X.M.; Jia, D.C.; Zhou, Y.; Yang, Z.H.; Wang, Y.J.; Ren, F.Q.; Yu, D.R.; Ding, Y.J. Mechanical properties and plasma erosion resistance of BNp/Al2O3-SiO2 composite ceramics. *J. Cent. South. Univ.* **2013**, *20*, 1462–1468, doi:10.1007/s11771-013-1635-3.

119. Levchenko, I.; Xu, S.; Teel, G.; Mariotti, D.; Walker, M.L.R.; Keidar, M. Recent progress and perspectives of space electric propulsion systems based on smart nanomaterials. *Nat. Commun.* **2018**, *9*, 879, doi:10.1038/s41467-017-02269-7.